Bioorganic Chemistry 45 (2012) 1–11

Contents lists available at SciVerse ScienceDirect

Bioorganic Chemistry

journal homepage: www.elsevier.com/locate/bioorg

Outstanding Paper

Selected C7-substituted chromone derivatives as monoamine oxidase inhibitors

Lesetja J. Legoabe [a], Anél Petzer [a], Jacobus P. Petzer [b,*]

[a] Unit for Drug Research and Development, School of Pharmacy, North-West University, Private Bag X6001, Potchefstroom 2520, South Africa
[b] Pharmaceutical Chemistry, School of Pharmacy, North-West University, Private Bag X6001, Potchefstroom 2520, South Africa

ARTICLE INFO

Article history:
Received 29 March 2012
Available online 31 August 2012

Keywords:
Monoamine oxidase
Inhibition
Reversible
Chromone
Coumarin
Structure–activity relationship

ABSTRACT

A series of C7-substituted chromone (1-benzopyran-4-one) derivatives were synthesized and evaluated as inhibitors of recombinant human monoamine oxidase (MAO) A and B. The chromones are structurally related to a series of C7-functionalized coumarin (1-benzopyran-2-one) derivatives which has been reported to act as potent MAO inhibitors. The results of the current study document that the chromones are highly potent reversible inhibitors of MAO-B with IC_{50} values ranging from 0.008 to 0.370 μM. While the chromone derivatives also exhibit affinities for MAO-A, with IC_{50} values ranging from 0.495 to 8.03 μM, they are selective for the MAO-B isoform. Structure–activity relationships (SAR) show that 7-benzyloxy substitution of chromone is suitable for MAO-B inhibition with tolerance for a variety of substituents and substitution patterns on the benzyloxy ring. It may be concluded that 7-benzyloxychromones are appropriate lead compounds for the design of reversible and selective MAO-B inhibitors. With the aid of modeling studies, potential binding orientations and interactions of selected chromone derivatives in the MAO-A and -B active sites are examined.

1. Introduction

The monoamine oxidases (MAO) are flavoenzymes which play an important role in the oxidative catabolism of amine neurotransmitters such as dopamine, serotonin and epinephrine [1]. All mammals contain two distinctive MAO enzymes, MAO-A and MAO-B, which are localized in the outer membrane of the mitochondria [2,3]. These enzymes are encoded by separate genes and share approximately 70% sequence identity at the amino acid level [3]. Based on the observation that the genes exhibit identical exon–intron organizations, it is thought that the two MAO genes evolved by duplication of a single ancestral gene [4]. Although the structures of the MAOs are highly similar, they exhibit different substrate and inhibitor specificities. Most notably, MAO-A utilizes serotonin as substrate while the dietary amines, β-phenylethylamine and benzylamine, are MAO-B selective substrates [5,6]. Dopamine, epinephrine and norepinephrine are considered to be substrates for both isoforms [1,5]. Relatively minor differences in the architectures of their respective active sites are thought to determine the observed differences in specificities of MAO-A and -B. The volume of the MAO-A active site is ~400 Å^3 while the MAO-B active site cavity has a volume of ~700 Å^3 [7,8]. While the MAO-A active site is a single cavity, the MAO-B active site consists of an entrance cavity (300 Å^3) which leads, from the surface of the enzyme, to the substrate cavity (~400 Å^3) [4]. Since the side chain of residue Ile-199 may adopt two different conformations, the active site of MAO-B may exist as two separate cavities or fuse into a large single cavity. The rotamer conformation of the Ile-199 side chain is determined by the nature of the bound ligand. With relatively large ligands bound to MAO-B, the side chain of Ile-199 rotates from the normally "closed" conformation into the "open" conformation. This allows for the fusion of the active site cavities, and is necessary for the accommodation of larger ligands [9]. The residue in MAO-A which corresponds to Ile-199 in MAO-B, is Phe-208. The increased bulk of the phenyl side chain of Phe-208 may impede the binding of larger MAO-B selective inhibitors to MAO-A. In contrast to the Ile-199 side chain, the side chain of Phe-208 residue in MAO-A does not adopt an alternate conformation. Based on these observations, the differences in size and conformational flexibility of Ile-199 and Phe-208 are determinants of the differential MAO-A and -B substrate and inhibitor specificities [4]. Another notable difference between the MAO-A and -B active sites involves a restriction imposed on the MAO-B active site by the phenolic ring of the Tyr-326 side chain. Residue Tyr-326 is found at the boundary between the substrate and entrance cavities of MAO-B and may obstruct certain ligands from adopting similar orientations to those observed in the MAO-A active site [7]. The corresponding residue to Tyr-326 in MAO-A, is Ile-335. The smaller size of the Ile-335 side chain allows for specific binding orientations in the MAO-A active

Abbreviations: DMSO, dimethyl sulfoxide; FAD, flavin adenine dinucleotide; MAO, monoamine oxidase; PDB, protein data bank; RMSD, root mean square deviation; SAR, structure–activity relationship; SI, selectivity index.

* Corresponding author. Fax: +27 18 2994243.
E-mail address: jacques.petzer@nwu.ac.za (J.P. Petzer).

0045-2068/$ - see front matter © 2012 Elsevier Inc. All rights reserved.
http://dx.doi.org/10.1016/j.bioorg.2012.08.003

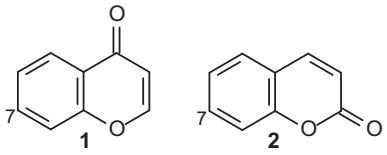

Fig. 1. The structures of chromone (**1**) and coumarin (**2**).

site which would not be possible in MAO-B. These structural differences may also be considered as determinants of the differential MAO-A and -B substrate and inhibitor specificities [4].

The MAO enzymes are of medical and pharmacological importance. Since MAO-A catalyzes the oxidation of central and peripheral serotonin, MAO-A inhibitors are used in the management of anxiety disorder and depression [5,10]. The finding that MAO-A levels exhibit an age-dependent increase in the hearts of rats, suggests that MAO-A may also play a role in cardiac cellular degeneration [11]. Since hydrogen peroxide is generated by the MAO catalytic cycle, increased levels of reactive oxygen species, derived from hydrogen peroxide, may lead to apoptosis and necrosis of cardiac cells. MAO-B inhibitors, in turn, are used in the therapy of Parkinson's disease [12]. MAO-B levels and activity exhibits an age-dependent increase in most brain regions, including the basal ganglia [13–15]. This increased MAO-B activity is expected to diminish dopamine levels and contribute to dopamine depletion in the parkinsonian brain. MAO-B inhibitors may therefore exert a dopamine sparing effect and are used as adjuvant therapy to levodopa, the metabolic precursor of dopamine. In accordance with this analysis, it has been demonstrated that, in primates, MAO-B inhibitors enhance dopamine levels derived from levodopa [16,17]. MAO-B inhibitors may also indirectly increase striatal extracellular dopamine levels by inhibiting the catabolism β-phenylethylamine. This increases the central levels of β-phenylethylamine which is both a releaser of dopamine as well as an inhibitor of active dopamine uptake [18]. Interestingly, MAO-B inhibitors may also protect against the neurodegenerative processes associated with Parkinson's disease by reducing the generation of hydrogen peroxide and dopanal [19]. These species are metabolic by-products of the MAO-B catalyzed oxidation of dopamine and may lead to neuronal damage when produced in excessive quantities in the brain [20–23]. Increased levels of hydrogen peroxide may promote apoptotic signaling events while dopanal has been implicated in α-synuclein aggregation [24]. Both these processes are thought to be involved in the development of Parkinson's disease.

Based on the pharmacological importance of MAO inhibitors, the design of new MAO inhibitors is pursued by several research groups. The present study aims to discover novel highly potent human MAO inhibitors by employing the chromone (1-benzopyran-4-one) structure as scaffold. Chromone (**1**) is a member of the benzopyrone class of compounds and a structural isomer of coumarin (1-benzopyran-2-one, **2**) (Fig. 1). Coumarins, in particular C7-functionalized coumarin derivatives, have been shown to act as potent reversible inhibitors of the MAO enzymes [25]. Substitution of coumarin and coumarin derivatives at C7 of the benzopyrone ring with the benzyloxy moiety yields compounds which are particularly potent and selective MAO-B inhibitors [25]. The present study investigated the possibility that C7 substitution of chromone may similarly lead to structures endowed with potent MAO inhibitory properties. For this purpose alkyloxy substituents – benzyloxy, phenylethoxy and phenylpropoxy – were selected for substitution at C7 of the chromone ring. To further examine the structure–activity relationships (SAR) for MAO inhibition, the first member of the present series, the 7-benzyloxychromone derivative (**3a**), was substituted on the benzyloxy phenyl ring with alkyl groups (CH_3, CN, CF_3) and halogens (Cl, Br, F) (Table 1). The view that the chromone ring may act as a scaffold for the design of MAO inhibitors is supported by recent reports of a subset of C2- and C3-substituted chromone derivatives which act as inhibitors of MAO-B [26,27]. A small series of C6- and C7-substituted chromones have also been found to be inhibitors of both MAO isozymes [25]. This research forms part of a recent study by us, which examined the MAO inhibitory properties of a series of C6-substituted chromones [28].

Table 1
The structures of the C7-substituted chromone derivatives (**3a**–**o**) that were examined in this study.

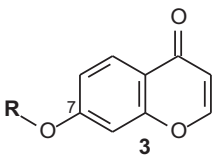

R	R	R	R
—CH_2— **a**	—$(CH_2)_2$— **b**	—$(CH_2)_3$— **c**	—CH_2— **d** (Cl)
—CH_2— **e** (Cl)	—CH_2— **f** (Br)	—CH_2— **g** (Br)	—CH_2— **h** (F)
—CH_2— **i** (F)	—CH_2— **j**	—CH_2— **k**	—CH_2— **l** (CN)
—CH_2— **m** (CN)	—CH_2— **n** (CF_3)	—$(CH_2)_2$— **o** (Br)	

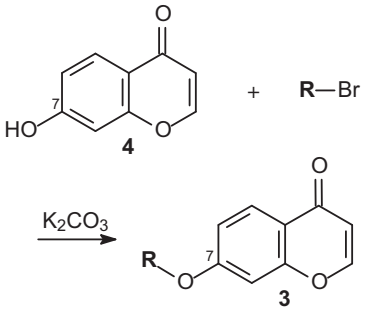

Scheme 1. Synthetic route to C7-substituted chromone derivatives (**3a**–**o**).

2. Results

2.1. Chemistry

The route followed for the synthesis of the target C7-substituted chromone derivatives (**3a**–**o**) is shown in Scheme 1 [28]. Compounds **3a**–**o** were synthesized in relatively good yields (25–84%) by reacting 7-hydroxy-4-chromone (**4**) with the appropriate alkyl bromides. These reactions were conducted in the presence of K_2CO_3, and acetone served as solvent. In most instances, the products were purified by recrystallization from ethanol. Compounds **3b** and **3o**, however, required purification by column chromatography as cited in Section 4. The structures and purities of the new compounds were verified by ^{1}H NMR, ^{13}C NMR, mass spectrometry and HPLC (see Section 4).

2.2. MAO inhibition studies

To examine the MAO-A and -B inhibitor properties of the C7-substituted chromone derivatives (**3a**–**o**), recombinant human MAO-A and -B were employed as enzyme sources. The mixed MAO-A/B substrate, kynuramine, was used for the enzyme activity measurements of both isozymes [29,30]. Kynuramine is oxidized by the MAO isozymes to yield 4-hydroxyquinoline which fluoresces in the alkaline medium used to terminate the enzymatic reactions. Using fluorescence spectrophotometry, the concentrations of 4-hydroxyquinoline in the reactions were measured without interference from kynuramine or the test inhibitors. From the rate data obtained in the presence of various concentrations of the test inhibitors, sigmoidal dose–response curves were constructed and the corresponding IC_{50} values were calculated (Fig. 2). All determinations were carried out in triplicate.

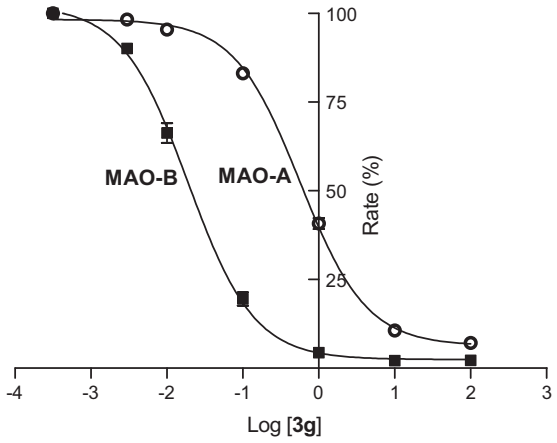

Fig. 2. The sigmoidal dose–response curves of the human MAO-A (circles) and MAO-B (squares) catalytic rates as a function of the logarithm of the concentration of inhibitor **3g** (expressed in μM). The determinations were carried out in triplicate and the values are given as mean ± SD.

Table 2
The IC_{50} values for the inhibition of recombinant human MAO-A and -B by the C7-substituted chromomes **3a**–**o**.

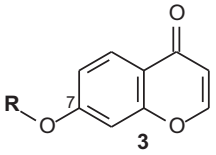

	R	IC_{50} (μM)[a]		SI[b]
		MAO-A	MAO-B	
3a	C_6H_5–CH_2–	5.33 ± 0.105	0.085 ± 0.005	63
3b	C_6H_5–$(CH_2)_2$–	2.19 ± 0.057	0.115 ± 0.003	19
3c	C_6H_5–$(CH_2)_3$–	3.08 ± 0.096	0.121 ± 0.018	25
3d	3-ClC_6H_4–CH_2–	1.52 ± 0.027	0.017 ± 0.002	89
3e	4-ClC_6H_4–CH_2–	0.495 ± 0.019	0.029 ± 0.005	17
3f	3-BrC_6H_4–CH_2–	1.73 ± 0.044	0.014 ± 0.001	124
3g	4-BrC_6H_4–CH_2–	0.592 ± 0.060	0.018 ± 0.005	33
3h	3-FC_6H_4–CH_2–	2.10 ± 0.153	0.044 ± 0.004	48
3i	4-FC_6H_4–CH_2–	1.17 ± 0.032	0.025 ± 0.002	47
3j	3-$CH_3C_6H_4$–CH_2–	8.03 ± 0.497	0.062 ± 0.008	130
3k	4-$CH_3C_6H_4$–CH_2–	7.12 ± 0.353	0.075 ± 0.002	95
3l	3-CNC_6H_4–CH_2–	0.784 ± 0.019	0.370 ± 0.033	2
3m	4-CNC_6H_4–CH_2–	1.57 ± 0.043	0.117 ± 0.002	13
3n	4-$CF_3C_6H_4$–CH_2–	1.97 ± 0.098	0.008 ± 0.002	246
3o	4-BrC_6H_4–$(CH_2)_2$–	0.718 ± 0.027	0.317 ± 0.028	2

[a] All values are expressed as the mean ± SD of triplicate determinations.
[b] The selectivity index is the selectivity for the MAO-B isoform and is given as the ratio of IC_{50}(MAO-A)/IC_{50}(MAO-B).

2.2.1. IC_{50} values for the inhibition of MAO-B

The IC_{50} values for the inhibition of MAO-B by the C7-substituted chromone derivatives **3a**–**o** are presented in Table 2. The results show that the chromones are highly potent inhibitors of human MAO-B with all of the recorded IC_{50} values in the nanomolar range. In accordance with literature reports that the benzyloxy side chain enhances the MAO inhibition potencies of coumarin derivatives [25], the present study finds that benzyloxy substitution of chromone at C7 also yields compounds with potent MAO-B inhibitory properties. For example, the first member of the series, the 7-benzyloxychromone derivative **3a**, exhibited an IC_{50} value of 0.085 μM. Extending the length of the C7 side chain of **3a** with methylene and ethylene units to yield the phenylethoxy (**3b**, IC_{50} = 0.115 μM) and phenylpropoxy (**3c**, IC_{50} = 0.121 μM) substituted homologues, respectively, resulted in a slight loss of MAO-B inhibition potency. Although not statistically significant ($p > 0.05$), from these results it may be concluded that benzyloxy substitution at C7 of chromone is more favorable for potent MAO-B inhibition than substitution with the phenylethoxy and phenylpropoxy moieties. Substitution on the benzyloxy phenyl ring of derivative **3a** with halogens leads to a relatively large enhancement of MAO-B inhibition potency. For example, *meta* and *para* substitution of **3a** with chlorine, bromine and fluorine yielded structures (**3d**–**i**) with IC_{50} values ranging from 0.014 to 0.044 μM. These derivatives are approximately two–sixfold more potent as MAO-B inhibitors than **3a** ($p < 0.05$ in all instances). Alkyl substitution on the benzyloxy phenyl ring of derivative **3a** also yielded structures with potent MAO-B inhibitory properties. For example, structures **3j**–**k**, the methyl substituted homologues, were more potent MAO-B inhibitors than the unsubstituted homologue **3a**, although by a small degree and not statistically significant ($p > 0.05$). Similarly,

the trifluoromethyl substituted homologue **3n** was also found to be more potent than **3a** ($p < 0.05$). In fact **3n** proved to be the most potent inhibitor of the present series with an IC_{50} value of 0.008 μM. Interestingly, the cyano substituted derivatives **3l**–**m** exhibited weaker MAO-B inhibitory potencies than the corresponding unsubstituted homologue **3a** (**3l**, $p < 0.05$; **3m**, $p > 0.05$). Among the chromone derivatives substituted with a benzyloxy moiety at C7, those containing cyano groups on the benzyloxy ring were the weakest MAO-B inhibitors. In spite of this, compounds **3l** and **3m** may still be viewed as potent MAO-B inhibitors with IC_{50} values of 0.370 μM and 0.117 μM, respectively. In accordance with the view that benzyloxy substitution at C7 of chromone is more favorable for MAO-B inhibition than phenylethoxy substitution (see above), *para* bromine substitution of the 7-phenylethoxychromone derivative **3b**, yielded structure **3o** (IC_{50} = 0.317 μM) which is approximately 17-fold weaker ($p < 0.05$) as an MAO-B inhibitor than the *para* bromine substituted 7-benzyloxychromone derivative **3g** (IC_{50} = 0.018 μM). Interestingly, *meta* and *para* substitution of a particular substituent (Cl, Br, F, CH_3) on **3a** yielded similar MAO-B inhibition activities for both positions ($p > 0.05$). The only exception is cyano substitution with the *para* substituted derivative, **3m** being 3-fold more potent than the corresponding *meta* substituted derivative **3l** ($p < 0.05$). This result shows that, for the most part, the substitution pattern has little effect on the MAO-B inhibitory potencies of 7-benzyloxychromone derivatives.

2.2.2. IC_{50} values for the inhibition of MAO-A

As shown in Table 2 the C7-substituted chromone derivatives **3a**–**o** are also inhibitors of human MAO-A. The IC_{50} values that were recorded for the series ranged from 0.495 to 8.03 μM. The selectivity index (SI) values indicated that the chromones are selective inhibitors of the MAO-B isozyme. The most selective compound, derivative **3n**, is also the most potent MAO-B inhibitor of the present series. In contrast to the results obtained with MAO-B, the phenylethoxy (**3b**, IC_{50} = 2.19 μM) and phenylpropoxy (**3c**, IC_{50} = 3.08 μM) substituted homologues were more potent MAO-A inhibitors than the 7-benzyloxychromone derivative **3a** (IC_{50} = 5.33 μM) ($p < 0.05$ in both instances). *Meta* and *para* substitution on the benzyloxy phenyl ring of derivative **3a** with halogen containing functional groups (Cl, Br, F, CF_3) and the cyano group led to an enhancement of MAO-A inhibition potency ($p < 0.05$ in all instances), with the homologue containing a *para* chlorine substituent, compound **3e**, exhibiting the most potent MAO-A inhibition of the series (IC_{50} = 0.495 μM). In contrast to the results obtained with MAO-B, methyl substitution on the benzyloxy ring of derivative **3a** was associated with reduced MAO-A inhibitory potency ($p < 0.05$ in both instances). For example, the derivatives substituted at the *meta* (**3j**) and *para* (**3k**) positions with the methyl group exhibited IC_{50} values of 8.03 μM and 7.12 μM, respectively. Interestingly, *para* bromine substitution of the 7-phenylethoxychromone derivative **3b**, to yield structure **3o** (IC_{50} = 0.718 μM), resulted in enhanced MAO-A inhibition compared to **3b** ($p < 0.05$). This result is dissimilar to that obtained with MAO-B since bromine substitution of **3b** leads to a decrease of MAO-B inhibition potency. Interestingly, for most 7-benzyloxychromone derivatives, *para* substitution of a particular substituent (Cl, Br, F, CH_3) yielded improved MAO-A inhibition ($p < 0.05$) compared to *meta* substitution. The only exception is cyano substitution with the *meta* substituted derivative, **3l** exhibiting 2-fold higher potency than the corresponding *para* substituted derivative **3m** ($p < 0.05$).

2.3. Reversibility of MAO inhibition

Literature reports that 7-benzyloxycoumarin derivatives are competitive inhibitors, and therefore reversible inhibitors, of rat MAO-A and -B [25]. To verify that 7-benzyloxychromone derivatives are also reversible inhibitors of MAO-A and -B, the reversibility of inhibition of a selected inhibitor of the present series, compound **3g**, was evaluated. Compound **3g** was selected as representative inhibitor since it displayed potent inhibition towards both MAO-A and -B. For the purpose of the reversibility study, the recoveries of the enzymatic activities after dilution of enzyme-inhibitor complexes were evaluated. The human MAO enzymes were firstly incubated with compound **3g** at concentrations of 10 × IC_{50} and 100 × IC_{50} for 30 min and then diluted 100-fold to yield concentrations of the inhibitor of 0.1 × IC_{50} and 1 × IC_{50}, respectively, and the residual enzyme catalytic rates were measured. As shown in Fig. 3, after dilution of **3g** to a concentration equal to 0.1 × IC_{50}, the MAO-A and -B activities were recovered to levels of 94% and 96% of the control values, respectively. This behavior is consistent with a reversible interaction of **3g** with MAO-A and -B. In contrast, after treatment of MAO-A and -B with the irreversible inhibitors, pargyline and (R)-deprenyl, respectively, enzyme activity is not regained.

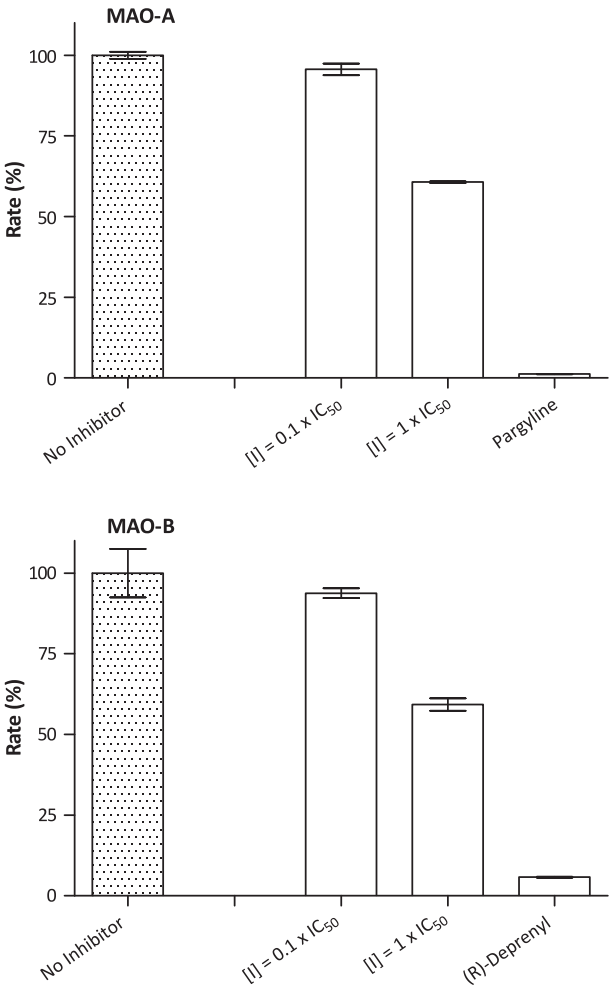

Fig. 3. Recovery of enzyme activity after dilution. MAO-A (top panel) and MAO-B (bottom panel) were preincubated with compound **3g** at concentrations equal to 10 × IC_{50} and 100 × IC_{50} for 30 min and then diluted to 0.1 × IC_{50} and 1 × IC_{50}, respectively. The residual enzyme activities were subsequently measured.

The possibility that **3g** acts as a competitive inhibitor of human MAO-A and -B was also investigated. Lineweaver–Burk double reciprocal plots for the catalytic activities of MAO-A and -B were constructed in the absence and presence of three different concentrations of **3g**. The results, shown in Fig. 4, document that the double reciprocal plots constructed with both MAO-A and -B

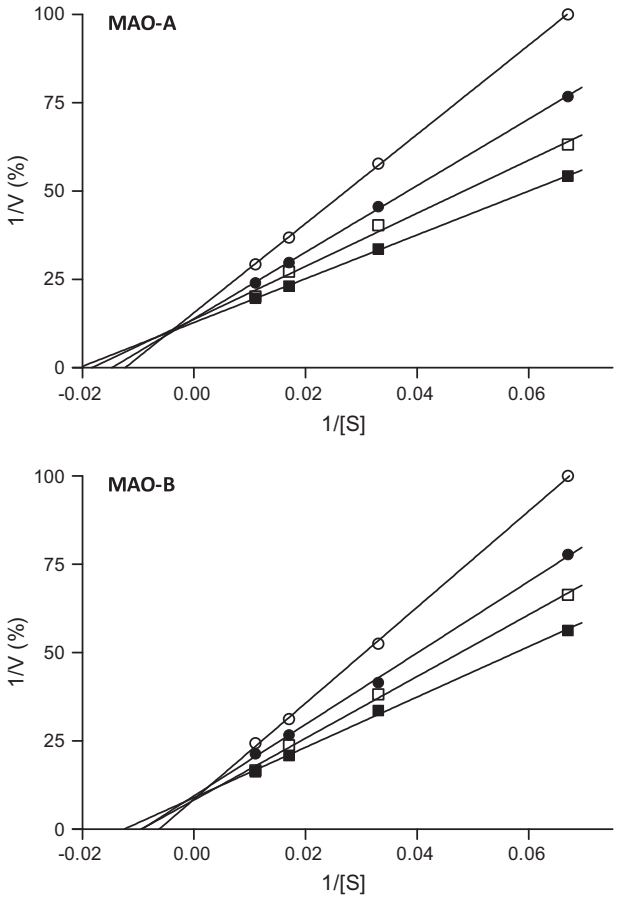

Fig. 4. A set of four Lineweaver–Burk plots were constructed for the oxidation of kynuramine by human MAO-A (top) and MAO-B (bottom). The data were collected in the absence (filled squares) and presence of three different concentrations of **3g**. The inhibitor concentrations selected for the MAO-A studies were 0.148 μM (open squares), 0.296 μM (filled circles) and 0.592 μM (open circles) while the inhibitor concentrations selected for the MAO-B studies were 0.0045 μM (open squares), 0.009 μM (filled circles), 0.018 μM (open circles).

are linear and each set has a common *y*-intercept. This behavior indicates that **3g** acts as a competitive inhibitor of human MAO-A and -B, and provides additional support for the finding that **3g** is a reversible MAO inhibitor.

2.4. Molecular modeling

As discussed in Section 1, the availability of the crystallographic structures of MAO-A and -B greatly assists in the design of inhibitors of these enzymes and may provide a structural rationale for the observed inhibitory properties of certain classes of compounds. To provide additional insight into the MAO inhibition modes of C7-substituted chromone derivatives, possible binding orientations and interactions of selected inhibitors, compounds **3g** and **3n**, were explored via molecular docking studies. For this purpose, the X-ray crystal structures of human MAO-A cocrystallized with harmine (PDB entry: 2Z5X) [7] and human MAO-B cocrystallized with 7-(3-chlorobenzyloxy)-4-formylcoumarin (PDB entry: 2V60) [31] served as protein models. The protein model of MAO-B is particularly suitable for the docking studies since this model would enable the comparison of the binding orientation of the coumarin moiety of the cocrystallized ligand with the chromone moieties of **3g** and **3n**. Furthermore, in this model the side chain of Ile-199 is rotated into the "open" conformation which allows for larger ligands, such as the chromone derivatives examined here, to fit into the MAO-B

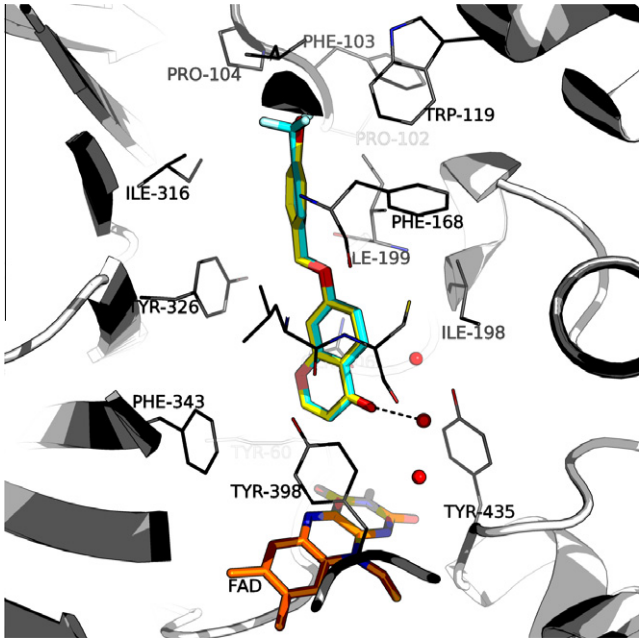

Fig. 5. The predicted binding orientations of **3g** (yellow) and **3n** (cyan) within the MAO-B active site. (For interpretation of the references to color in this figure legend, the reader is referred to the web version of this article.)

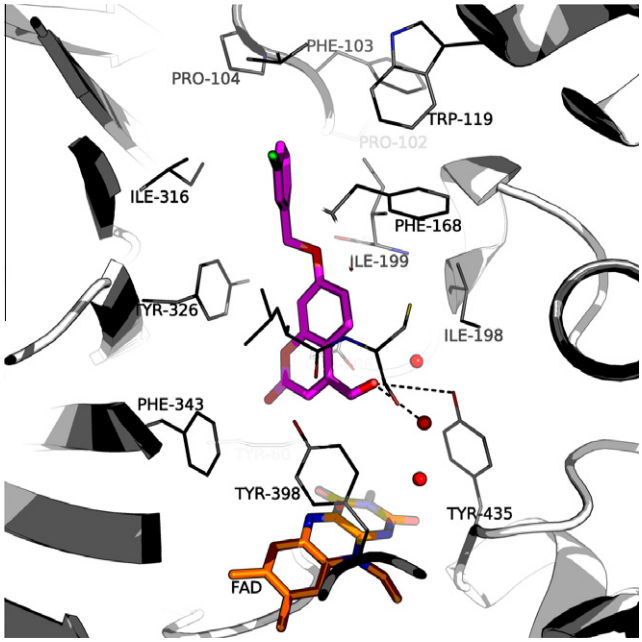

Fig. 6. The reported three-dimensional structure of 7-(3-chlorobenzyloxy)-4-formylcoumarin in complex with the human MAO-B active site (2V60.pdb) [31].

active site. The preparation of the models and the docking calculations were carried out with the Windows based Discovery Studio 3.1 modeling software (Accelrys) [32] according to the literature procedure [28,33]. The CDOCKER module of Discovery Studio 3.1 was utilized for the docking calculations. This docking protocol has been shown to be appropriate for predicting binding orientations of ligands in the active sites of MAO-A and -B [28].

The highest ranked docking orientation of compound **3g** in the active site of the MAO-B model is illustrated in Fig. 5. The 10 highest ranked solutions display similar binding orientations with

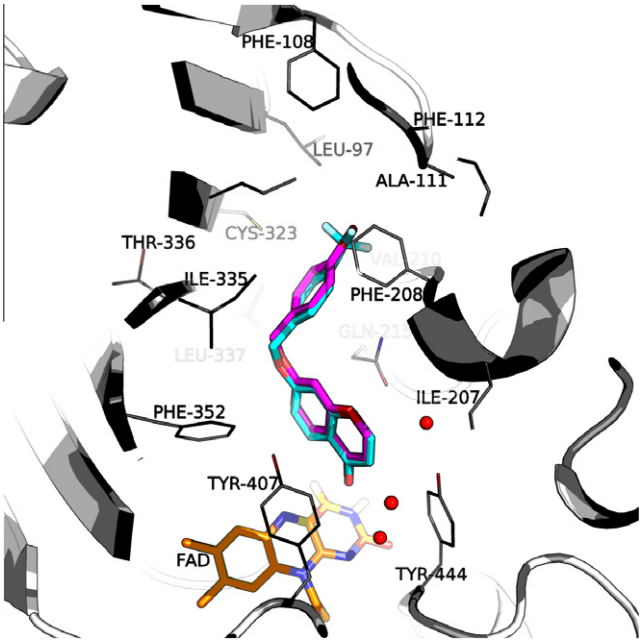

Fig. 7. The predicted binding orientations of **3g** (purple) and **3n** (cyan) within the MAO-A active site. (For interpretation of the references to color in this figure legend, the reader is referred to the web version of this article.)

RMSD values of less than 0.21 Å from the position of the best ranked solution. The chromone moiety of **3g** is located within the substrate cavity of the enzyme, in close proximity of the flavin adenine dinucleotide (FAD) cofactor. The orientation and binding position of the chromone are similar to that of the coumarin ring of the cocrystallized ligand (Fig. 6) [31]. This binding position of **3g** may allow for the formation of a π–π interaction (5.2 Å) between the chromone ring and the aromatic ring of Tyr-398. In addition, the benzopyrone carbonyl oxygen of **3g** is within hydrogen bond distance to an active site water molecule. The formyl carbonyl oxygen of the cocrystallized ligand, which binds in the same region as the benzopyrone carbonyl oxygen of **3g**, is reported to also undergo a hydrogen bond interaction with this water molecule. Also similar to the cocrystallized ligand, the C7 side chain of **3g** extends into the entrance cavity of the MAO-B active site. Since the entrance cavity is reported to be a highly hydrophobic environment, the C7 substituents are stabilized principally by Van der Waals interactions within the entrance cavity [34].

The highest ranked docking orientation of compound **3g** in the active site of the MAO-A model is illustrated in Fig. 7. Compound **3g** exhibits a similar binding orientation in the MAO-A active site to that observed in MAO-B. The chromone moiety of **3g** binds in the proximity of the FAD cofactor with the C7 benzyloxy side chain extending towards the entrance of the active site. A hydrogen on the benzyloxy ring of **3g** may undergo a potential π–σ interaction with the phenyl ring of Phe-208. Interestingly, **3g** binds in a folded conformation in the MAO-A active site, while exhibiting an extended conformation in the MAO-B active site. As discussed in Section 1, the increased bulk of the phenyl side chain of Phe-208 may impede the binding of relatively large inhibitors in the MAO-A active site. To avoid structural overlap with Phe-208 in the MAO-A active site, larger inhibitors bind in a folded conformation. The ability of the side chain of Ile-199 to rotate from the MAO-B active site cavity enables larger inhibitors to bind in an extended conformation in MAO-B. The differences in size and conformational flexibility of Ile-199 and Phe-208 may therefore explain the different binding modes of **3g** to MAO-A and -B [4]. Assuming that the extended conformation results in more productive interactions with the active site residues compared to the folded conformation, the ability of the C7-substituted chromone derivatives to bind in an extended conformation to MAO-B may explain their selective inhibition of the MAO-B isozyme. The assumption that the extended conformation is more favorable for MAO-B inhibition is in accordance to the observation that inhibitors, which span both active site cavities, are frequently more potent inhibitors than those binding only in the substrate cavity [9].

It is noteworthy that in both MAO-A and -B, compound **3n** exhibits virtually identical binding modes to **3g**. This suggests that not many differences in the binding orientations of the 7-benzyloxychromone class of compounds exist and explain the similar MAO-A and -B inhibitory activities among these derivatives.

3. Discussion and conclusion

The present study examined the MAO inhibitory properties of a series of C7-substituted chromones and finds that these compounds are highly potent inhibitors of human MAO-B. For comparison, the reversible MAO-B inhibitor safinamide exhibits an IC_{50} value of 0.08–0.5 μM, and 6-benzyloxychromone inhibits MAO-B with an IC_{50} value of 0.053 μM (SI = 62) under similar conditions [28,31]. The results further document that a representative member of the series acts reversibly in a competitive manner. Among the compounds studied, benzyloxy substitution of chromone is the most favorable for MAO-B inhibition. The effects on MAO-B inhibition by different substituents and substitution patterns on the benzyloxy ring of 7-benzyloxychromone were also examined. With the exception of cyano substitution, all substitution and substitution patterns enhanced MAO-B inhibition potency. The modeling studies propose that the C7-substituted chromones bind to both active site cavities of MAO-B with the C7 side chain occupying the entrance cavity while the chromone moiety binds within the in substrate cavity. Since the entrance cavity is reported to be a highly hydrophobic space, it may be expected that an enhancement of the lipophilicity of the C7 side chain will result in more productive Van der Waals interactions with the entrance cavity, and thus an enhancement in binding affinity [34]. Substitution on the benzyloxy phenyl ring with halogens and alkyl groups will increase the lipophilicity of the C7 side chain, and may explain the observed enhancements of MAO-B inhibition potencies compared to the unsubstituted homologue **3a**.

C7-substituted chromones are also inhibitors of human MAO-A. All compounds, however, display selective inhibition of MAO-B, with the most potent MAO-B inhibitor, compound **3n**, exhibiting a 246-fold selectivity for MAO-B. Analyses of the predicted binding orientations and interactions of a representative chromone, compound **3g**, in the MAO-A and -B active sites show that the chromone moiety of **3g** may undergo π–π interactions and hydrogen bonding within the MAO-B active site while, in MAO-A, these interactions are predicted not to occur. The absence of these potentially stabilizing interactions in MAO-A may explain the lower MAO-A inhibition potencies of the chromones compared to their potencies for the inhibition of MAO-B. The modeling studies also suggest that, while **3g** binds in an extended conformation in the MAO-B active site, it adopts a folded conformation in MAO-A. Compared to the folded conformation, the extended conformation may place the benzyloxy phenyl ring in a more favorable position/orientation to undergo productive interactions in the hydrophobic entrance cavity space. This may contribute to the selective inhibition of the MAO-B isozyme by the C7-substituted chromones. Another dissimilarity between the binding orientations of **3g** within MAO-A and -B is the orientation of the chromone moiety within the substrate cavity. Compared to its orientation in MAO-B, the chromone ring of **3g** is

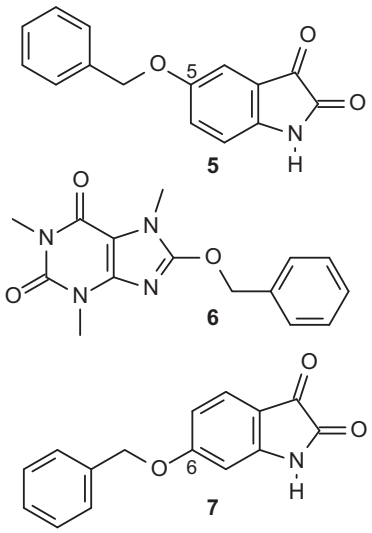

Fig. 8. The structures of 5-benzyloxyisatin (**5**), 8-benzyloxycaffeine (**6**) and 6-benzyloxyisatin (**7**).

rotated through ~180° in MAO-A. This places the benzopyrone carbonyl oxygen in a region in the MAO-A substrate cavity where the oxygen is predicted not to undergo hydrogen bonding. In contrast, in MAO-B, the benzopyrone carbonyl oxygen is directed towards a water molecule with which hydrogen bonding is predicted to occur. The potential formation of this stabilizing hydrogen bond interaction may explain, at least in part, the higher inhibition potencies of the chromones for MAO-B. The finding that fused aromatic moieties exhibit differing orientations in the MAO-A and -B active sites is in agreement with literature which reports that, in the MAO-B substrate cavity, the isatin ring of the reversible MAO inhibitor, 5-benzyloxyisatin (**5**), may also be rotated through ~180° compared to its position in MAO-A (Fig. 8) [35]. Similarly modeling studies have shown that in MAO-B, the caffeine ring of 8-benzyloxycaffeine (**6**) may also be rotated through ~180° compared to its position in MAO-A [30]. Interestingly, the modeling studies indicate that inhibitors **3g** and **3n** exhibits highly similar binding orientations to both MAO-A and -B. In spite of this, compound **3n** displays a much larger degree of MAO-B inhibition and selectivity than **3g**. While the molecular reasons for this are unclear, a possible explanation may be that the CF_3 group of **3n** (σ_p = 0.54), by virtue of its higher Hammett constant (σ_p), forms more productive interactions with the MAO-B active site than the **3g** bromine (σ_p = 0.23) [30]. It has previously been demonstrated that the MAO-B inhibitory activities of a series of 8-benzyloxycaffeines correlates with increasing σ values [30]. In contrast, MAO-A inhibition does not correlate with σ [30].

As mentioned in Section 1, we have recently reported the MAO inhibitory properties of a series of C6-substituted chromones [28]. Compared to the C6-substituted chromones, which exhibited IC_{50} values for the inhibition of human MAO-B of 0.002–0.076 μM, the C7-substituted homologues (IC_{50} = 0.008–0.370 μM) may be considered as less potent inhibitors. For example, the C6-substituted homologue of **3n** was found to be a fourfold more potent inhibitor than **3n** (IC_{50} = 0.008 μM) with an IC_{50} value of 0.002 μM. Interestingly, modeling studies indicate that C6-substituted chromones exhibit similar binding modes in the MAO-B active site compared to the C7-substituted chromones [28]. The principal difference is that, the chromone rings of the C6-substituted chromones are rotated by ~180° compared to the orientations of the C7-substituted homologues (Fig. 9). This finding is similar to a previous report that, in the MAO-B substrate cavity, the isatin moiety of the reversible MAO inhibitor, 5-benzyloxyisatin (**5**), may also be rotated through

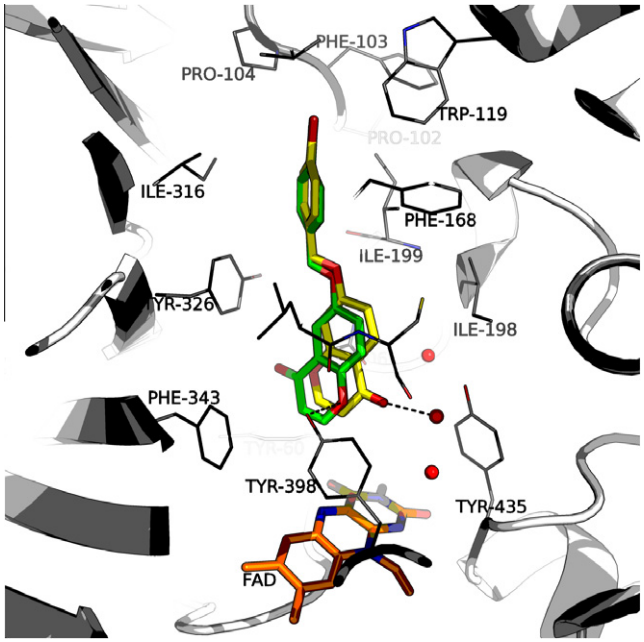

Fig. 9. A comparison of the predicted binding orientations of **3g** and its C6-substituted homologue within the MAO-B active site.

~180° compared to the orientation of the isatin moiety of the 6-benzyloxyisatin isomer (**7**) [35]. These data suggest that the binding orientation adopted by the chromone ring in the MAO-B substrate cavity is determined by the position of the substituent. For optimal placement of a C7 substituent in the entrance cavity, the chromone ring adopts a different binding orientation in the substrate cavity compared to the orientation of the chromone rings of C6-substituted homologues. Since the C6-substituted chromones are more potent MAO-B inhibitors than the C7-substituted chromones, it may be concluded that the binding mode of the C6-substituted homologues allows for more productive interactions with the MAO-B active site. Among these is a potential hydrogen bond with Tyr-398 which is predicted to occur with the C6-substituted chromones, but not the C7-substituted chromones [28].

4. Experimental section

4.1. Chemicals and instrumentation

Unless otherwise noted, the reagents required for the chemical synthesis were acquired from Sigma–Aldrich and were used without purification. Proton (^1H) and carbon (^{13}C) NMR spectra were recorded on a Bruker Avance III 600 spectrometer at frequencies of 600 MHz and 150 MHz, respectively. All NMR measurements were conducted in $CDCl_3$ containing tetramethylsilane. Chemical shifts are given in parts per million (δ) downfield from the signal of tetramethylsilane. Spin multiplicities are reported as s (singlet), d (doublet), dd (doublet of doublets), t (triplet), q (quartet) or m (multiplet). Direct insertion high resolution mass spectra (HRMS) were obtained on a DFS high resolution magnetic sector mass spectrometer (Thermo Electron Corporation) in electron ionization (EI) mode. Melting points (mp) were measured with a Buchi M-545 melting point apparatus and are uncorrected. The purities of the final synthesized products were evaluated by HPLC analyses which were conducted with an Agilent 1100 HPLC system equipped with a quaternary pump and an Agilent 1100 series diode array detector (see Supplementary material). HPLC grade acetonitrile (Merck) and Milli-Q water (Millipore) was used for the chromatography.

Fluorescence spectrophotometry was carried out with a Varian Cary Eclipse fluorescence spectrophotometer. Microsomes from insect cells containing recombinant human MAO-A and -B (5 mg/mL) and kynuramine.2HBr were from Sigma–Aldrich.

4.2. Synthesis of the C7 substituted chromone derivatives (**3a–o**)

7-Hydroxy-4-chromone (3 mmol) was dissolved in 20 ml of acetone. To this solution, anhydrous potassium carbonate (6 mmol) and the appropriate alkyl bromide (6 mmol) were added, and the reaction mixture was heated at reflux and stirred for 24 h. The reaction was filtered through a pad of Celite and the solvent was subsequently removed in vacuo. The crude residue was triturated with 50 mL diethyl ether, the resulting solid material was collected by filtration and dried overnight at 60 °C. Compounds **3b** and **3o** required column chromatographic purification. For these compounds, the residue obtained after removal of the reaction solvent was chromatographed using neutral alumina as stationary phase and dichloromethane-ethylacetate (4:1) as an eluent. The chromone derivatives were recrystallized from ethanol.

4.2.1. 7-(Benzyloxy)-4H-chromen-4-one (**3a**)

The title compound (light orange powder) was prepared by reacting 7-hydroxychromone and benzyl bromide in acetone, with a yield of 49%: mp 129.2–130.3 °C (ethanol). ^{1}H NMR (Bruker Avance III, 600 MHz, $CDCl_3$) δ 8.10 (d, J = 8.9 Hz, 1H), 7.74 (d, J = 6.0 Hz, 1H), 7.45–7.30 (m, 5H), 7.02 (dd, J = 8.9, 2.4 Hz, 1H), 6.89 (d, J = 2.4 Hz, 1H), 6.25 (d, J = 6.0 Hz, 1H), 5.13 (s, 2H). ^{13}C NMR (Bruker Avance III, 150 MHz, $CDCl_3$) δ 176.93, 163.06, 158.09, 154.80, 135.59, 128.73, 128.38, 127.47, 127.23, 118.91, 114.95, 112.91, 101.43, 70.48. HRMS *m*/*z*: calcd for $C_{16}H_{12}O_3$, 252.0786, found 252.0793. Purity (HPLC): 99%.

4.2.2. 7-(2-Phenylethoxy)-4H-chromen-4-one (**3b**)

The title compound (white powder) was prepared by reacting 7-hydroxychromone and 2-phenylethyl bromide in acetone, with a yield of 34%: mp 86.8–89.7 °C (ethanol). ^{1}H NMR (Bruker Avance III, 600 MHz, $CDCl_3$) δ 8.07 (d, J = 8.9 Hz, 1H), 7.73 (d, J = 5.9 Hz, 1H), 7.36–7.21 (m, 5H), 6.94 (dd, J = 8.9, 2.3 Hz, 1H), 6.79 (d, J = 2.3 Hz, 1H), 6.24 (d, J = 6.0 Hz, 1H), 4.23 (t, J = 7.0 Hz, 2H), 3.12 (t, J = 7.0 Hz, 2H). ^{13}C NMR (Bruker Avance III, 150 MHz, $CDCl_3$) δ 176.95, 163.21, 158.13, 154.77, 137.52, 128.93, 128.56, 127.13, 126.71, 118.72, 114.75, 112.88, 100.90, 69.20, 35.43. HRMS *m*/*z*: calcd for $C_{17}H_{14}O_3$, 266.0942, found 266.0938. Purity (HPLC): 99%.

4.2.3. 7-(3-Phenylpropoxy)-4H-chromen-4-one (**3c**)

The title compound (cream colored powder) was prepared by reacting 7-hydroxychromone and 3-phenylpropyl bromide in acetone, with a yield of 68%: mp 93.1–94.0 °C (ethanol). ^{1}H NMR (Bruker Avance III, 600 MHz, $CDCl_3$) δ 8.09 (d, J = 8.9 Hz, 1H), 7.75 (d, J = 6.0 Hz, 1H), 7.28 (m, 2H), 7.19 (m, 3H), 6.95 (dd, J = 8.9, 2.4 Hz, 1H), 6.78 (d, J = 2.4 Hz, 1H), 6.25 (d, J = 6.0 Hz, 1H), 4.01 (t, J = 6.2 Hz, 2H), 2.81 (t, J = 7.5 Hz, 2H), 2.19–2.10 (m, 2H). ^{13}C NMR (Bruker Avance III, 150 MHz, $CDCl_3$) δ 177.03, 163.49, 158.20, 154.79, 140.97, 128.48, 128.45, 127.14, 126.08, 118.66, 114.80, 112.89, 100.84, 67.46, 31.96, 30.43. HRMS *m*/*z*: calcd for $C_{18}H_{16}O_3$, 280.1099, found 280.1099. Purity (HPLC): 99%.

4.2.4. 7-[(3-Chlorobenzyl)oxy]-4H-chromen-4-one (**3d**)

The title compound (brown powder) was prepared by reacting 7-hydroxychromone and 3-chlorobenzyl bromide in acetone, with a yield of 77%: mp 136.8–137.0 °C (ethanol). ^{1}H NMR (Bruker Avance III, 600 MHz, $CDCl_3$) δ 8.11 (d, J = 9.0 Hz, 1H), 7.75 (d, J = 6.0 Hz, 1H), 7.42 (d, J = 1.9 Hz, 1H), 7.35–7.26 (m, 3H), 7.02 (dd, J = 8.9, 2.4 Hz, 1H), 6.87 (d, J = 2.4 Hz, 1H), 6.25 (d, J = 6.0 Hz, 1H), 5.10 (s, 2H). ^{13}C NMR (Bruker Avance III, 150 MHz, $CDCl_3$) δ 176.88, 162.69, 158.05, 154.84, 137.64, 134.67, 130.02, 128.51, 127.40, 127.38, 125.34, 119.12, 114.81, 112.96, 101.49, 69.56. HRMS *m*/*z*: calcd for $C_{16}H_{11}ClO_3$, 286.0397, found 286.0395. Purity (HPLC): 99%.

4.2.5. 7-[(4-Chlorobenzyl)oxy]-4H-chromen-4-one (**3e**)

The title compound (brown powder) was prepared by reacting 7-hydroxychromone and 4-chlorobenzyl bromide in acetone, with a yield of 73%: mp 126.1–127.3 °C (ethanol). ^{1}H NMR (Bruker Avance III, 600 MHz, $CDCl_3$) δ 8.09 (d, J = 8.8 Hz, 1H), 7.74 (d, J = 5.9 Hz, 1H), 7.35 (s, 4H), 7.00 (d, J = 8.9 Hz, 1H), 6.86 (s, 1H), 6.25 (d, J = 5.9 Hz, 1H), 5.09 (s, 2H). ^{13}C NMR (Bruker Avance III, 150 MHz, $CDCl_3$) δ 176.87, 162.76, 158.04, 154.83, 134.22, 134.09, 128.91, 128.77, 127.33, 119.04, 114.84, 112.94, 101.45, 69.66. HRMS *m*/*z*: calcd for $C_{16}H_{11}ClO_3$, 286.0397, found 286.0395. Purity (HPLC): 99%.

4.2.6. 7-[(3-Bromobenzyl)oxy]-4H-chromen-4-one (**3f**)

The title compound (white powder) was prepared by reacting 7-hydroxychromone and 3-bromobenzyl bromide in acetone, with a yield of 82%: mp 145.4–145.5 °C (ethanol). ^{1}H NMR (Bruker Avance III, 600 MHz, $CDCl_3$) δ 8.11 (d, J = 8.9 Hz, 1H), 7.75 (d, J = 6.1 Hz, 1H), 7.58 (t, J = 1.8 Hz, 1H), 7.47 (d, J = 8.0 Hz, 1H), 7.34 (d, J = 7.8 Hz, 1H), 7.29–7.22 (m, 1H), 7.02 (dd, J = 8.9, 2.4 Hz, 1H), 6.87 (d, J = 2.4 Hz, 1H), 6.26 (d, J = 6.0 Hz, 1H), 5.08 (s, 2H). ^{13}C NMR (Bruker Avance III, 150 MHz, $CDCl_3$) δ 176.90, 162.69, 158.06, 154.86, 137.90, 131.46, 130.33, 130.30, 127.41, 125.84, 122.82, 119.14, 114.82, 112.98, 101.50, 69.51. HRMS *m*/*z*: calcd for $C_{16}H_{11}BrO_3$, 329.9892, found 329.9889. Purity (HPLC): 99%.

4.2.7. 7-[(4-Bromobenzyl)oxy]-4H-chromen-4-one (**3g**)

The title compound (light brown powder) was prepared by reacting 7-hydroxychromone and 4-bromobenzyl bromide in acetone, with a yield of 84%: mp 139.7–139.8 °C (ethanol). ^{1}H NMR (Bruker Avance III, 600 MHz, $CDCl_3$) δ 8.21 (d, J = 6.0 Hz, 1H), 7.94 (d, J = 8.8 Hz, 1H), 7.61 (d, J = 8.3 Hz, 2H), 7.44 (d, J = 8.4 Hz, 2H), 7.21 (d, J = 2.4 Hz, 1H), 7.12 (dd, J = 8.8, 2.4 Hz, 1H), 6.27 (d, J = 6.0 Hz, 1H), 5.23 (s, 2H). ^{13}C NMR (Bruker Avance III, 150 MHz, $CDCl_3$) δ 175.64, 162.51, 157.64, 156.52, 135.55, 131.48, 130.04, 126.48, 121.32, 118.28, 115.12, 112.19, 101.87, 69.19. HRMS *m*/*z*: calcd for $C_{16}H_{11}BrO_3$, 329.9892, found 329.9885. Purity (HPLC): 99%.

4.2.8. 7-[(3-Fluorobenzyl)oxy]-4H-chromen-4-one (**3h**)

The title compound (brown powder) was prepared by reacting 7-hydroxychromone and 3-fluorobenzyl bromide in acetone, with a yield of 70%: mp 180.6–181.8 °C (ethanol). ^{1}H NMR (Bruker Avance III, 600 MHz, $CDCl_3$) δ 8.11 (d, J = 8.8 Hz, 1H), 7.75 (d, J = 5.8 Hz, 1H), 7.35 (q, J = 7.2 Hz, 1H), 7.19 (d, J = 7.5 Hz, 1H), 7.14 (d, J = 9.4 Hz, 1H), 7.03 (m, 2H), 6.87 (s, 1H), 6.26 (d, J = 5.9 Hz, 1H), 5.13 (s, 2H). ^{13}C NMR (Bruker Avance III, 150 MHz, $CDCl_3$) δ 176.90, 163.79, 162.74, 162.15, 158.07, 154.85, 138.20, 130.37, 130.32, 127.39, 122.72, 119.12, 115.35, 115.21, 114.84, 114.32, 114.17, 112.97, 101.52, 69.62. HRMS *m*/*z*: calcd for $C_{16}H_{11}FO_3$, 270.0692, found 270.0681. Purity (HPLC): 99%.

4.2.9. 7-[(4-Fluorobenzyl)oxy]-4H-chromen-4-one (**3i**)

The title compound (brown powder) was prepared by reacting 7-hydroxychromone and 4-fluorobenzyl bromide in acetone, with a yield of 67%: mp 120.6–121.3 °C (ethanol). ^{1}H NMR (Bruker Avance III, 600 MHz, $CDCl_3$) δ 8.09 (d, J = 8.9 Hz, 1H), 7.74 (d, J = 5.8 Hz, 1H), 7.42–7.37 (m, 2H), 7.07 (t, J = 8.2 Hz, 2H), 7.00 (d, J = 8.9 Hz, 1H), 6.87 (s, 1H), 6.25 (d, J = 5.9 Hz, 1H), 5.08 (s, 2H). ^{13}C NMR (Bruker Avance III, 150 MHz, $CDCl_3$) δ 176.89, 162.85, 161.83, 158.06, 154.83, 131.38, 131.36, 129.43, 129.38, 127.29,

118.99, 115.75, 115.61, 114.86, 112.92, 101.42, 69.79. HRMS *m*/*z*: calcd for $C_{16}H_{11}FO_3$, 270.0692, found 270.0694. Purity (HPLC): 99%.

*4.2.10. 7-[(3-Methylbenzyl)oxy]-4H-chromen-4-one (**3j**)*

The title compound (brown powder) was prepared by reacting 7-hydroxychromone and 3-methylbenzyl bromide in acetone, with a yield of 73%: mp 89.0–91.8 °C (ethanol). ^{1}H NMR (Bruker Avance III, 600 MHz, $CDCl_3$) δ 8.14 (d, J = 9.2 Hz, 1H), 7.79 (d, J = 6.0 Hz, 1H), 7.35–7.25 (m, 3H), 7.20 (d, J = 7.5 Hz, 1H), 7.07 (dd, J = 8.9, 2.3 Hz, 1H), 6.93 (s, 1H), 6.29 (d, J = 6.0 Hz, 1H), 5.13 (s, 2H), 2.41 (s, 3H). ^{13}C NMR (Bruker Avance III, 150 MHz, $CDCl_3$) δ 176.94, 163.13, 158.10, 154.79, 138.48, 135.49, 129.14, 128.62, 128.21, 127.20, 124.58, 118.87, 114.96, 112.90, 101.40, 70.56, 21.38. HRMS *m*/*z*: calcd for $C_{17}H_{14}O_3$, 266.0943, found 266.0937. Purity (HPLC): 99%.

*4.2.11. 7-[(4-Methylbenzyl)oxy]-4H-chromen-4-one (**3k**)*

The title compound (light pink powder) was prepared by reacting 7-hydroxychromone and 4-methylbenzyl bromide in acetone, with a yield of 67%: mp 118.2–119.3 °C (ethanol). ^{1}H NMR (Bruker Avance III, 600 MHz, $CDCl_3$) δ 8.09 (d, J = 8.9 Hz, 1H), 7.74 (d, J = 5.8 Hz, 1H), 7.31 (d, J = 7.5 Hz, 2H), 7.19 (d, J = 7.6 Hz, 2H), 7.01 (d, J = 8.9 Hz, 1H), 6.88 (s, 1H), 6.25 (d, J = 5.9 Hz, 1H), 5.08 (s, 2H), 2.35 (s, 3H). ^{13}C NMR (Bruker Avance III, 150 MHz, $CDCl_3$) δ 176.94, 163.14, 158.09, 154.78, 138.26, 132.53, 129.39, 127.62, 127.17, 118.83, 114.99, 112.88, 101.39, 70.45, 21.18. HRMS *m*/*z*: calcd for $C_{17}H_{14}O_3$, 266.0943, found 299.0929. Purity (HPLC): 99%.

*4.2.12. 3-{[(4-Oxo-4H-chromen-7-yl)oxy]methyl}benzonitrile (**3l**)*

The title compound (brown crystals) was prepared by reacting 7-hydroxychromone and 3-cyanobenzyl bromide in acetone, with a yield of 66%: mp 156.8–157.0 °C (ethanol). ^{1}H NMR (Bruker Avance III, 600 MHz, $CDCl_3$) δ 8.11 (d, J = 8.5 Hz, 1H), 7.76 (d, J = 5.6 Hz, 1H), 7.23 (s, 1H), 7.66 (d, J = 7.5 Hz, 1H), 7.62 (d, J = 7.5 Hz, 1H), 7.51 (t, J = 7.8 Hz, 1H), 7.01 (d, J = 9.0 Hz, 1H), 6.87 (s, 1H), 6.25 (d, J = 6.0 Hz, 1H), 5.15 (s, 2H). ^{13}C NMR (Bruker Avance III, 150 MHz, $CDCl_3$) δ 176.79, 162.35, 157.99, 154.90, 137.26, 131.92, 131.46, 130.66, 129.56, 127.49, 119.28, 118.36, 114.63, 112.97, 112.91, 101.53, 69.04. HRMS *m*/*z*: calcd for $C_{17}H_{11}NO_3$, 277.0739, found 277.0733. Purity (HPLC): 99%.

*4.2.13. 4-{[(4-Oxo-4H-chromen-7-yl)oxy]methyl}benzonitrile (**3m**)*

The title compound (orange powder) was prepared by reacting 7-hydroxychromone and 4-cyanobenzyl bromide in acetone, with a yield of 68%: mp 213.7–213.8 °C (ethanol). ^{1}H NMR (Bruker Avance III, 600 MHz, $CDCl_3$) δ 8.11 (d, J = 8.9 Hz, 1H), 7.75 (d, J = 6.1 Hz, 1H), 7.68 (d, J = 7.8 Hz, 2H), 7.54 (d, J = 7.9 Hz, 2H), 7.02 (d, J = 8.9 Hz, 1H), 6.86 (s, 1H), 6.26 (d, J = 5.9 Hz, 1H), 5.19 (s, 2H). ^{13}C NMR (Bruker Avance III, 150 MHz, $CDCl_3$) δ 176.78, 162.36, 158.00, 154.89, 140.97, 132.52, 127.56, 127.52, 119.30, 118.43, 114.66, 113.00, 112.16, 101.54, 69.27. HRMS *m*/*z*: calcd for $C_{17}H_{11}NO_3$, 277.0739, found 277.0733. Purity (HPLC): 99%.

*4.2.14. 7-{[4-(Trifluoromethyl)benzyl]oxy}-4H-chromen-4-one (**3n**)*

The title compound (brown powder) was prepared by reacting 7-hydroxychromone and 4-(trifluoromethyl)benzyl bromide in acetone, with a yield of 69%: mp 159.3–159.4 °C (ethanol). ^{1}H NMR (Bruker Avance III, 600 MHz, $CDCl_3$) δ 8.11 (d, J = 8.9 Hz, 1H), 7.75 (d, J = 5.9 Hz, 1H), 7.65 (d, J = 7.8 Hz, 2H), 7.54 (d, J = 7.8 Hz, 2H), 7.02 (d, J = 8.9 Hz, 1H), 6.87 (s, 1H), 6.25 (d, J = 5.9 Hz, 1H), 5.19 (s, 2H). ^{13}C NMR (Bruker Avance III, 150 MHz, $CDCl_3$) δ 176.86, 162.61, 158.05, 154.87, 139.66, 130.63, 130.42, 127.44, 127.40, 125.71 (q), 124.83, 123.02, 119.19, 114.78, 112.98, 101.51, 69.52. HRMS *m*/*z*: calcd for $C_{17}H_{11}F_3O_3$, 320.0660, found 320.0659. Purity (HPLC): 99%.

*4.2.15. 7-[2-(4-Bromophenyl)ethoxy]-4H-chromen-4-one (**3o**)*

The title compound (white powder) was prepared by reacting 7-hydroxychromone and 4-bromophenethyl bromide in acetone, with a yield of 25%: mp 93.1–93.8 °C (ethanol). ^{1}H NMR (Bruker Avance III, 600 MHz, $CDCl_3$) δ 8.07 (d, J = 8.9 Hz, 1H), 7.74 (d, J = 6.0 Hz, 1H), 7.43 (d, J = 8.3 Hz, 2H), 7.15 (d, J = 8.3 Hz, 2H), 6.92 (dd, J = 8.9, 2.4 Hz, 1H), 6.78 (d, J = 2.4 Hz, 1H), 6.24 (d, J = 6.0 Hz, 1H), 4.20 (t, J = 6.7 Hz, 2H), 3.07 (t, J = 6.7 Hz, 2H). ^{13}C NMR (Bruker Avance III, 150 MHz, $CDCl_3$) δ 176.92, 163.04, 158.11, 154.80, 136.63, 131.63, 130.67, 127.22, 120.60, 118.84, 114.66, 112.92, 100.94, 68.77, 34.85. HRMS *m*/*z*: calcd for $C_{17}H_{13}BrO_3$, 344.0048, found 344.0033. Purity (HPLC): 99%.

4.3. Human MAO inhibition studies

Microsomes from insect cells containing recombinant human MAO-A and -B were obtained from commercial sources (Sigma–Aldrich). The enzymatic reactions were conducted in potassium phosphate buffer (100 mM, pH 7.4, made isotonic with KCl 20.2 mM) to a final volume of 500 μL, and contained kynuramine (45 μM for MAO-A and 30 μM for MAO-B), various concentrations of the test inhibitors (0–100 μM) and 4% DMSO as cosolvent. The reactions were initiated by the addition of MAO-A or -B (0.0075 mg protein/mL) and were subsequently incubated for 20 min at 37 °C. The reactions were terminated by the addition of 400 μL NaOH (2 N) and 1000 μL water, centrifuged for 10 min at 16,000*g* and the concentrations of 4-hydroxyquinoline in the supernatants were measured spectrofluorometrically (λ_{ex} = 310 - nm; λ_{em} = 400 nm) [29,33,36]. A linear calibration curve was constructed by preparing samples containing 4-hydroxyquinoline (0.047–1.56 μM) dissolved in 500 μL potassium phosphate buffer. To each calibration standard, volumes of 400 μL NaOH (2 N) and 1000 μL water were added. The appropriate control samples were included to confirm that the test inhibitors do not fluoresce or quench the fluorescence of 4-hydroxyquinoline under these assay conditions. IC_{50} values were estimated from sigmoidal dose–response curves (graphs of the initial rate of kynuramine oxidation versus the logarithm of inhibitor concentration). Each sigmoidal curve was constructed from six different inhibitor concentrations spanning at least three orders of magnitude. Data analyses were carried out with the Prism 5 software package (GraphPad) employing the one site competition model. IC_{50} values were determined in triplicate and are expressed as mean ± standard deviation (SD). One-way analyses of variances (ANOVA) with Tukey's post hoc test was used to determine if statistical differences exist between the means of the IC_{50} values among the test compounds.

4.4. Recovery of enzyme activity after dilution

Compound **3g** at concentrations equal to $10 \times IC_{50}$ and $100 \times IC_{50}$ for the inhibition of the respective MAO isozymes was preincubated with recombinant human MAO-A or -B (0.75 mg/ml) for 30 min at 37 °C in potassium phosphate buffer (100 mM, pH 7.4, made isotonic with KCl). Control incubations were conducted in the absence of inhibitor, and DMSO (4%) was added as co-solvent to all preincubations. The reactions were subsequently diluted 100-fold with the addition of a solution of kynuramine to yield final concentrations of compound **3g** equal to $0.1 \times IC_{50}$ and $1 \times IC_{50}$. The final concentrations of kynuramine were 45 μM and 30 μM for MAO-A and -B, respectively, and the final concentrations of MAO-A and -B were 0.0075 mg/mL. The reactions were incubated for a further 20 min at 37 °C, terminated and the residual rates of 4-hydroxyquinoline formation were measured as described above. The residual enzyme catalytic rates were expressed as mean ± SD. As control experiments, pargyline (IC_{50} = 12.97 μM) and (R)-deprenyl (IC_{50} = 0.079 μM) were similarly preincubated with

recombinant human MAO-A and -B (0.75 mg/ml) at concentrations equal to 100 × IC_{50} and diluted 100-fold with the addition of kynuramine to yield final concentrations of the inhibitors equal to 1 × IC_{50} [37].

4.5. Lineweaver–Burk plots

A set consisting of four Lineweaver–Burk plots were constructed for the inhibition of recombinant human MAO-A and -B by the selected inhibitor **3g**. For this purpose, the rates of kynuramine oxidation by MAO-A and -B were measured in the absence and presence of three different concentrations of **3g**. The enzymatic reactions were conducted as described above and contained kynuramine (15–90 μM), the test inhibitor (0.148–0.592 μM for MAO-A and 0.0045–0.018 μM for MAO-B) and 4% DMSO as cosolvent. The reactions were initiated by the addition of MAO-A or -B (0.015 mg protein/mL). The rate measurements were carried out as described above. Linear regression analysis was performed using GraphPad Prism 5 [35].

4.6. Modeling studies

Molecular modeling was carried out with the Windows based Discovery Studio 3.1 software (Accelrys) [32]. Models of the X-ray crystal structures of human MAO-A (PDB code, 2Z5X) [7] and human MAO-B (PDB code, 2V60) [31] were obtained from the Brookhaven Protein Data Bank. The pKa values and protonation states of the ionizable amino acids were calculated and hydrogen atoms were added at pH 7.4 to the protein models. The correctness of the valences of the FAD cofactors (oxidized state) and cocrystallized ligands were verified, the protein models were automatically typed with the Momany and Rone CHARMm forcefield and a fixed atom constraint was applied to the backbone. The models were subsequently energy minimized using the Smart Minimizer algorithm with the maximum amount of steps set to 50,000. The implicit generalized Born solvation model with molecular volume was used during the minimization procedure. The cocrystallized ligands, waters and the backbone constraints were removed from the models and the binding sites were identified from an analysis of the enzyme cavities. In each model, three active site waters are considered to be conserved and were retained. These waters are HOH 710, 718 and 739 in the MAO-A active site, and HOH 1159, 1166 and 1309 in the A-chain of the MAO-B active site. The structures of compounds **3g** and **3n** were drawn in Discovery Studio and their geometries were briefly optimized using a Dreiding-like forcefield (5000 iterations). Atom potential types and partial charges were assigned with the Momany and Rone CHARMm forcefield. Docking of **3g** and **3n** into the protein models were subsequently carried out with the CDOCKER algorithm. For this purpose, ten random ligand conformations were generated, the heating target temperature was set to 700 K and full potential mode was employed. The docking solutions were finally refined using in situ ligand minimization with the Smart Minimizer algorithm. Unless otherwise specified, all the applications within Discovery Studio were set to their default values. The illustrations were generated with PyMOL [38].

Acknowledgments

The NMR spectra were recorded by André Joubert of the SASOL Centre for Chemistry, North-West University while the MS spectra were recorded by Marelize Ferreira of the Mass Spectrometry Service, University of the Witwatersrand. This work was supported by the North-West University and grants from the National Research Foundation and the Medical Research Council, South Africa.

Appendix A. Supplementary material

Supplementary data associated with this article can be found, in the online version, at http://dx.doi.org/10.1016/j.bioorg.2012.08.003.

References

[1] M.B.H. Youdim, Y.S. Bakhle, Monoamine oxidase: isoforms and inhibitors in Parkinson's disease and depressive illness, Br. J. Pharmacol. 147 (2006) S287–S296.
[2] A.W. Bach, N.C. Lan, D.L. Johnson, C.W. Abell, M.E. Bembenek, S.W. Kwan, P.H. Seeburg, J.C. Shih, CDNA cloning of human liver monoamine oxidase A and B: molecular basis of differences in enzymatic properties, Proc. Natl. Acad. Sci. USA 85 (1988) 4934–4939.
[3] J.C. Shih, K. Chen, M.J. Ridd, Monoamine oxidase: from genes to behavior, Annu. Rev. Neurosci. 22 (1999) 197–217.
[4] D.E. Edmondson, C. Binda, J. Wang, A.K. Upadhyay, A. Mattevi, Molecular and mechanistic properties of the membrane-bound mitochondrial monoamine oxidases, Biochemistry 48 (2009) 4220–4230.
[5] M.B.H. Youdim, D.E. Edmondson, K.F. Tipton, The therapeutic potential of monoamine oxidase inhibitors, Nat. Rev. Neurosci. 7 (2006) 295–309.
[6] A.A. Boulton, Phenylethylaminergic modulation of catecholaminergic neurotransmission, Prog. Neuropsychopharmacol. Biol. Psychiatry 15 (1991) 139–156.
[7] S.-Y. Son, J. Ma, Y. Kondou, M. Yoshimura, E. Yamashita, T. Tsukihara, Structure of human monoamine oxidase A at 2.2-A resolution: the control of opening the entry for substrates/inhibitors, Proc. Natl. Acad. Sci. USA 105 (2008) 5739–5744.
[8] C. Binda, P. Newton-Vinson, F. Hubálek, D.E. Edmondson, A. Mattevi, Structure of human monoamine oxidase B, a drug target for the treatment of neurological disorders, Nat. Struct. Biol. 9 (2002) 22–26.
[9] F. Hubálek, C. Binda, A. Khalil, M. Li, A. Mattevi, N. Castagnoli, D.E. Edmondson, Demonstration of isoleucine 199 as a structural determinant for the selective inhibition of human monoamine oxidase B by specific reversible inhibitors, J. Biol. Chem. 280 (2005) 15761–15766.
[10] S.E. Zisook, Clinical overview of monoamine oxidase inhibitors, Psychosomatics 26 (1985) 240–251.
[11] A. Maurel, C. Hernandez, O. Kunduzova, G. Bompart, C. Cambon, A. Parini, B. Francés, Age-dependent increase in hydrogen peroxide production by cardiac monoamine oxidase A in rats, Am. J. Physiol. Heart Circ. Physiol. 284 (2003) H1460–H1467.
[12] H.H. Fernandez, J.J. Chen, Monoamine oxidase-B inhibition in the treatment of Parkinson's disease, Pharmacotherapy 27 (2007) 174S–185S.
[13] A. Nicotra, F. Pierucci, H. Parvez, O. Santori, Monoamine oxidase expression during development and aging, Neurotoxicology 25 (2004) 155–165.
[14] J.S. Fowler, N.D. Volkow, G.J. Wang, J. Logan, N. Pappas, C. Shea, R. MacGregor, Age-related increases in brain monoamine oxidase B in living healthy human subjects, Neurobiol. Aging 18 (1997) 431–435.
[15] R.N. Kalaria, M.J. Mitchell, S.I. Harik, Monoamine oxidases of the human brain and liver, Brain 111 (1988) 1441–1451.
[16] J.P. Finberg, J. Wang, K. Bankiewich, J. Harvey-White, I.J. Kopin, D.S. Goldstein, Increased striatal dopamine production from L-DOPA following selective inhibition of monoamine oxidase B by R(+)-N-propargyl-1-aminoindan (rasagiline) in the monkey, J. Neural Transm. Suppl. 52 (1998) 279–285.
[17] D.A. Di Monte, L.E. DeLanney, I. Irwin, J.E. Royland, P. Chan, M.W. Jacowec, J.W. Langston, Monoamine oxidase-dependent metabolism of dopamine in the striatum and substantia nigra of L-DOPA-treated monkeys, Brain Res. 738 (1996) 53–59.
[18] J.P. Finberg, I. Lamensdorf, T. Armoni, Modification of dopamine release by selective inhibitors of MAO-B, Neurobiology (Bp) 8 (2000) 137–142.
[19] P.A. LeWitt, D.C. Taylor, Protection against Parkinson's disease progression: clinical experience, Neurotherapeutics 5 (2008) 210–225.
[20] M. Gesi, A. Santinami, R. Ruffoli, G. Conti, F. Fornai, Novel aspects of dopamine oxidative metabolism (confounding outcomes take place of certainties, Pharmacol. Toxicol. 89 (2001) 217–224.
[21] S.A. Marchitti, R.A. Deitrich, V. Vasiliou, Neurotoxicity and metabolism of the catecholamine-derived 3,4-dihydroxyphenylacetaldehyde and 3,4-dihydroxyphenylglycolaldehyde: the role of aldehyde dehydrogenase, Pharmacol. Rev. 59 (2007) 125–150.
[22] B. Halliwell, Reactive oxygen species and the central nervous system, J. Neurochem. 59 (1992) 1609–1623.
[23] I. Lamensdorf, G. Eisenhofer, J. Harvey-White, A. Nechustan, K. Kirk, I.J. Kopin, 3,4-Dihydroxyphenylacetaldehyde potentiates the toxic effects of metabolic stress in PC12 cells, Brain Res. 868 (2000) 191–201.
[24] J.K. Mallajosyula, D. Kaur, S.J. Chinta, S. Rajagopalan, A. Rane, D.G. Nicholls, D.A. Di Monte, H. Macarthur, J.K. Andersen, MAO B elevation in mouse brain astrocytes results in Parkinson's pathology, PLoS ONE 3 (2008) e1616.
[25] C. Gnerre, M. Catto, F. Leonetti, P. Weber, P.-A. Carrupt, C. Altomare, A. Carotti, B. Testa, Inhibition of monoamine oxidases by functionalized coumarin derivatives: biological activities, QSARs, and 3D-QSARs, J. Med. Chem. 43 (2000) 4747–4758.

[26] A. Gaspar, T. Silva, M. Yáñez, D. Viña, F. Orallo, F. Ortuso, E. Uriarte, S. Alcaro, F. Borges, Chromone, a privileged scaffold for the development of monoamine oxidase inhibitors, J. Med. Chem. 54 (2011) 5165–5173.
[27] A. Gaspar, J. Reis, A. Fonseca, N. Milhazes, D. Viña, E. Uriarte, F. Borges, Chromone 3-phenylcarboxamides as potent and selective MAO-B inhibitors, Bioorg. Med. Chem. Lett. 21 (2011) 707–709.
[28] L.J. Legoaba, A. Petzer, J.P. Petzer, Inhibition of monoamine oxidase by selected C6-substituted chromone derivatives, Eur. J. Med. Chem. 49 (2012) 343–353.
[29] L. Novaroli, M. Reist, E. Favre, A. Carotti, M. Catto, P.A. Carrupt, Human recombinant monoamine oxidase B as reliable and efficient enzyme source for inhibitor screening, Bioorg. Med. Chem. 13 (2005) 6212–6217.
[30] B. Strydom, S.F. Malan, N. Castagnoli Jr., J.J. Bergh, J.P. Petzer, Inhibition of monoamine oxidase by 8-benzyloxycaffeine analogues, Bioorg. Med. Chem. 18 (2010) 1018–1028.
[31] C. Binda, J. Wang, L. Pisani, C. Caccia, A. Carotti, P. Salvati, D.E. Edmondson, A. Mattevi, Structures of human monoamine oxidase B complexes with selective noncovalent inhibitors: safinamide and coumarin analogs, J. Med. Chem. 50 (2007) 5848–5852.
[32] Accelrys Discovery Studio 1.7, Accelrys Software Inc., San Diego, CA, USA, 2006. <http://www.accelrys.com>.
[33] B. Strydom, J.J. Bergh, J.P. Petzer, 8-Aryl- and alkyloxycaffeine analogues as inhibitors of monoamine oxidase, Eur. J. Med. Chem. 46 (2011) 3474–3485.
[34] L. Novaroli, A. Daina, E. Favre, J. Bravo, A. Carotti, F. Leonetti, M. Catto, P.A. Carrupt, M. Reist, Impact of species-dependent differences on screening, design, and development of MAO B inhibitors, J. Med. Chem. 49 (2006) 6264–6272.
[35] C.I. Manley-King, J.J. Bergh, J.P. Petzer, Inhibition of monoamine oxidase by selected C5- and C6-substituted isatin analogues, Bioorg. Med. Chem. 19 (2011) 261–274.
[36] H.P. Booysen, C. Moraal, G. Terre'Blanche, A. Petzer, J.J. Bergh, J.P. Petzer, Thio- and aminocaffeine analogues as inhibitors of human monoamine oxidase, Bioorg. Med. Chem. 19 (2011) 7507–7518.
[37] A. Petzer, B.H. Harvey, G. Wegener, J.P. Petzer, Azure B, a metabolite of methylene blue, is a high-potency, reversible inhibitor of monoamine oxidase, Toxicol. Appl. Pharm. 258 (2012) 403–409.
[38] W.L. DeLano, The PyMOL Molecular Graphics System, DeLano Scientific, San Carlos, USA, 2002.